

Multiple T-S States for Estuaries, Shelves, and Marginal Seas

J. A. WHITEHEAD¹

*Department of Physical Oceanography
Woods Hole Oceanographic Institution
MS #21, 360 Woods Hole Road
Woods Hole, Massachusetts 02543*

ABSTRACT: Simple theoretical box-models and laboratory experiments demonstrate that an estuary subjected to freshwater flux and heating or cooling can possess more than one stable, stationary state if a well-defined set of forcing conditions are present. Two types of estuaries can develop such multiple temperature-salinity states. The same may be true of continental shelves and marginal seas. One type receives freshwater runoff from land but is cooled in the winter. The second has net freshwater loss from evaporation but also receives strong solar heating. Criteria are found which define the conditions needed for multiple states. It is shown that under most conditions, the density difference between estuary and ocean would be dominated by salinity if the inlet is sufficiently small (such as inland seas). In contrast, if the inlet is sufficiently wide and atmospheric cooling and heating is sufficiently great, the density difference would be dominated by temperature. Multiple states lie between these extremes. One of the multiple states is dominated by the salinity difference between estuary and ocean, the other by temperature difference. Each state is stable.

Introduction

A continent generally produces a freshwater flux to the sides of the ocean because of freshwater outflow from precipitation. The freshwater flux is principally from rivers and varies in magnitude enormously along coasts, depending on the watershed geometry of each individual region. Naturally, this means that the magnitude of salinity in estuaries, bays, and along continental shelves ranges between 0‰ and the ocean value of approximately 35‰. Thus, worldwide there is enormous opportunity for flows to be driven strongly by salinity differences.

Continents also produce air that is colder than the ocean water at certain locations and times. For instance, during the coldest winter season the greatest heat fluxes from ocean to air are found near the western edge of the subtropical gyres. Landward of these gyres are large estuarine regions that receive intense cooling. In general, there are large stretches of ocean coastline whose waters are made less dense by freshwater run-off but more dense by cooling.

There are also some coastal regions with an opposite tendency for salinity and temperature. The lack of rivers and precipitation in desert regions can make the coastal water saltier and hence denser than offshore, but the warm atmosphere and strong solar heating can make the water warmer and less dense. This may happen seasonally.

It can be anticipated that a density decrease by freshwater accumulation accompanied by density

increase from surface cooling is abundantly found in winter for coasts of continents in excess of roughly 30° latitude in both hemispheres. For example, possible locations would be found along the east coast of North America north of Florida, the west coast of Europe north of Spain, the east coast of South America from the Rio de la Plata south, the west coast of South America in excess of 30°S, the west coast of Europe north of Spain, the northern coast of the Mediterranean Sea, the east coast of Asia from Korea north (and possibly from Hokkaido north in the outer islands), the west coast of North America north of Oregon, and all of the lands bordering the polar oceans. Examples of salt water accumulation accompanied by heating would probably be found near desert coastlines. Examples can most likely be found along the coasts of Africa away from the equatorial rain belts, around Australia, possibly near the equatorial region in the west South American coast, and along the western coasts along the Mexican and California coasts of North America.

The classification scheme formulated by Hansen and Rattray (1966) differentiates the buoyancy-driven estuary as one extreme from the tidal-driven estuary as the other. We are concerned here with the buoyancy-driven estuary in cases where both temperature and salinity play a role. In most reviews (Ippen 1966; Kennish 1986; Kjerfve 1988) there are no examples where salinity and temperature effects counteract each other to produce the effects to be discussed here, but they might clearly exist in some estuaries. To our knowledge, such effects are not presently considered in dynamic models of estuaries.

¹ Tele: 508-289-2793; Fax: 508-457-2181; e-mail: jwhitehead@whoi.edu.

A variety of examples of estuaries driven by the assorted types of buoyancy forcings are known. Chesapeake and Delaware bays are obvious large-scale examples where river runoff leads to low salinity water whose balance is maintained by exchange at their mouths. Funka Bay in Hokkaido, Japan, exhibits cold water removal through its mouth in winter with negligible salinity difference (Miyake et al. 1988). Spencer Gulf, South Australia (Bye and Whitehead 1975) exhibits high salinity due to evaporation, and apparently there is a steady balance of outflow of saline water and inflow of fresher ocean water at the mouth. In Prandle (1992) numerous other examples of either thermally or salinity dominated estuaries are presented. Examples are described in Jervis Bay, Australia, Loch Sunart, Scotland, Tamar Estuary, England, Naples Bay, Florida, Palmiet Estuary, South Africa, Weeks Bay, Alabama, St. Lawrence Estuary, Canada, and the Kattegat in the North-Baltic Sea transition region. Usually, the emphasis in the studies was upon the interaction of the stratified density field with waves or mixing, and either a salinity- or temperature-dominated field was found to be alone representative of density.

In Van Diemen Gulf, North Australia, both salinity and temperature changes were found to be important as one moved from the South Alligator River, through the saline gulf (from evaporation) into the thermally stratified Arafura Sea (Wolanski 1988). Although temperature effects are close to comparable to density effects, it appears to be in a salt-driven state.

The effects we are concerned with originated first in models of global ocean circulation driven by both differential heating and a freshwater flux (as the coastal waters are). It was found that values of temperature and salinity may adopt either one of two possible steady states if the boundary conditions lie within a certain parameter range (Stommel 1961, see also reviews by Weaver and Hughes 1992, Marotzke 1994, and Whitehead 1995). One state is characterized from equator to pole by a large density variation from salinity difference and by a smaller (and opposite) density variation from temperature difference. The other state is characterized by an even smaller density change from temperature difference and an almost negligible salinity difference. The present oceans are thought to occupy the second state.

This model is one of the simplest physical examples of finite amplitude instability for dynamic systems. But it has additional features that make it particularly important scientifically, as it shows that the large-scale ocean circulation could take two very different states for the same atmospheric forcing: One state being salinity driven with sinking at

the evaporative equatorial regions and rising at the rainy poles, and the other being the present state, with cold water sinking in polar regions and warm water rising near the equator. Only recently has this model been produced and investigated in a physical system (Whitehead 1996).

The purpose of this paper is to show that such multiple states are possible in estuarine and coastal regions. We have recently shown that the two boxes used in previous box-model studies (one equator-one pole) are not needed, one box next to a fixed ocean still can possess two stable states. This is demonstrated with equations for a simple one-box model and also with a laboratory experiment. This motivates the main purpose of this study: to clarify the criteria that are needed for the existence of two possible states in estuarine systems.

Let us sketch as an example, an idealized estuary driven by atmospheric cooling from temperature difference, ΔT^* , and subject also to freshwater flux, F^* . For ΔT^* that is zero or small, and F^* set at a fixed value, the estuary is driven by rising of the fresh water in the estuary and outflow of the fresh water at the top of the mouth (Fig. 1, top). For progressively greater ΔT^* , the freshwater driving will continue, but the speed of flushing will decrease since temperature forces oppose the salinity driving. We will review the way the fluid, in a fixed range of values of forcing, say $\Delta T_1^* < \Delta T^* < \Delta T_2^*$ can adopt both the above mode as well as a thermally-driven mode with sinking in the estuary. Both modes (Fig. 1, middle two panels) are stable and steady. In the salinity-driven mode, the overturning is slow. Temperature is almost saturated at ΔT^* but is unable to counteract the freshwater forcing. In the temperature-driven mode, overturning is more rapid: temperature is less saturated, and the salinity difference between estuary and ocean is quite small. The two modes are possible because temperature has a different response time than salinity in the estuary. For $\Delta T^* > \Delta T_2^*$, only the thermally-driven mode (Fig. 1, bottom) can exist.

We need to understand criteria such as the temperature ranges given above in order to locate and understand regions with two possible states. A region that can adopt either of two possible states may exhibit confusing behavior to someone who doesn't realize that either state is possible given the same climate forcing. One could imagine that an estuary might remain in the freshwater-driven mode for many months (or years), only to flip to the thermally-driven mode when something changes slightly for the next couple of months or years. Without guidance about the properties of such systems, a biologist or chemist might be hard pressed to understand the large changes in tem-

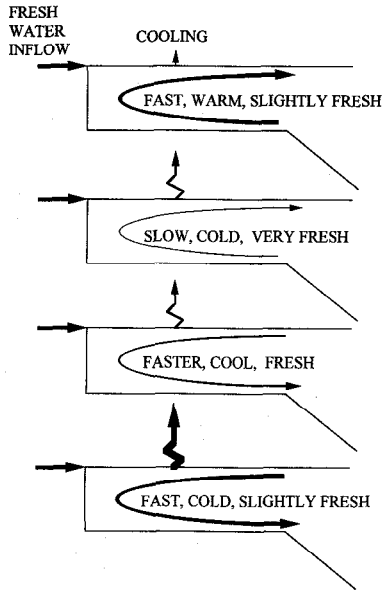


Fig. 1. Sketch four possible states that exist for a doubly driven estuary next to a warm, salty ocean from a constant value of freshwater runoff (straight arrows) and three successively greater rates of surface cooling (jagged arrows). For small cooling (top) the freshwater rises in the estuary and exits at the top. For greater cooling (2nd down), the density increase from cooling opposes the decrease from freshness, so the overturning cell is slower. In such a circumstance the temperature can be almost saturated but low salinity of the water dominates density. At the same rate of cooling (3rd down) the convection can have reverse sign so that faster flow with sinking of estuarine water due to its cold temperature can be found. The lowered salinity provides some opposition to the thermal forcing, but is largely overwhelmed by the rapid flushing. Finally, for great cooling (bottom) the thermal forcing creates a circulation that is so rapid that salinity of the water is changed very little.

perature and salinity that estuaries sometimes exhibit. The possible devastating effects on organisms and the challenges to predicting the state of the estuaries using improperly designed models is obvious.

In the section Formulation the simplest balance between the ocean and a region subject to both freshwater- and temperature-forcing is formulated. This leads to two criteria needed for multiple solutions. The first criterion expresses the role of the relative strength between the freshwater- and temperature-forcing. This criterion is obvious and discussed in the current reviews by Weaver and Hughes (1992), Marotzke (1994), and Whitehead (1995). The second criterion expresses the role of the strength of motion between the estuary and the deep ocean. It is not discussed in present reviews of multiple states. We seek to elucidate and more clearly quantify the second criterion here. It will become apparent that if the strength of motion is weak between the region and the ocean, only the freshwater mode can exist. For very strong

motion the temperature mode is strongly favored, although both modes are possible.

In view of the artificially of box and layered models used to date, and no matter how convincing they appear, it is important to verify that such behavior physically exists, either in an actual physical experiment or in nature. In the section A Laboratory Experiment a laboratory example is reviewed. The design of the apparatus illustrates the importance of the strength of motion between estuary and ocean. It also enables us to properly quantify the system so one can find examples of multiple states in nature. Some quantifiable criteria are developed and discussed in the section Consequences.

Formulation

Consider an estuary (which could also be thought of as a continental shelf or marginal sea) of surface area A and average depth D ($=V/A$ where V is volume) that is subjected to an atmosphere of temperature T^* and inflow of water with volume flux q , temperature T^* , and salinity S^* . The estuary is connected to the ocean whose temperature is T_0 and salinity is S_0 , and there is an inflow from ocean to the estuary of volume flux Q and outflow $Q + q$. As with box models of this problem, the water in the estuary is considered to be well mixed. The magnitude of Q or its relation to forcing parameters, such as wind stress, tides, or density difference between the estuary and ocean, will remain unspecified at this stage. We seek to predict temperature T' and salinity S' of the estuary water given values of q , S^* , T_0 , S_0 , and Q . The equations are

$$V \frac{dS'}{dt} = qS^* - (|Q| + q)S' + |Q|S_0 \quad (2.1)$$

$$V\rho C_p \frac{dT'}{dt} = \frac{kA}{\delta} [T^* - T'] - \rho C_p [(|Q| + q)T' - |Q|T_0 - qT^*] \quad (2.2)$$

where ρ is density and C_p is specific heat of water, k is conductivity of air, and δ is boundary layer thickness of the air. It is convenient to rearrange and simplify to:

$$\frac{dS}{dt} = \frac{1}{\tau_S} (S^{**} - S) - \frac{|Q|}{V} S \quad (2.3)$$

$$\frac{dT}{dt} = \frac{1}{\tau_T} [T^{**} - T] - \frac{|Q|}{V} T \quad (2.4)$$

where

$$\tau_S = \frac{V}{q} \quad (2.5)$$

$$\tau_T = \left[\frac{k}{\delta D \rho C_p} + \frac{q}{V} \right]^{-1} \quad (2.6)$$

$$S = S' - S_0, \quad T = T' - T_0,$$

$$S^{**} = S^* - S_0, \quad T^{**} = T^* - T_0$$

For a given value of Q , the value of S and T will approach fixed values that are

$$S = \frac{S^{**}}{1 + \frac{|Q|\tau_S}{V}} \quad (2.7)$$

$$T = \frac{T^{**}}{1 + \frac{|Q|\tau_T}{V}} \quad (2.8)$$

Let us assume that the relative density difference between the estuary and the ocean is expressed by the sum

$$\frac{\Delta \rho}{\rho} = \frac{\Delta \rho_S}{\rho} + \frac{\Delta \rho_T}{\rho} \quad (2.9)$$

using linear relations

$$\frac{\Delta \rho_T}{\rho} = -\alpha T$$

$$\frac{\Delta \rho_S}{\rho} = \beta S$$

so that

$$\frac{\Delta \rho}{\rho} = \beta S - \alpha T \quad (2.10)$$

and with α and β both positive we have

$$\frac{\Delta \rho}{\rho} = \frac{\beta S^{**}}{1 + \frac{|Q|\tau_S}{V}} - \frac{\alpha T^{**}}{1 + \frac{|Q|\tau_T}{V}} \quad (2.11)$$

The individual density differences due to salinity and temperature and their sum as a function of Q/V are sketched in Fig. 2 for the case of positive T^{**} and S^{**} where τ_T is smaller than τ_S by a factor of ten or so and αT^{**} is about the same size as βS^{**} . Just as in all of the preceding studies of multiple box models (Whitehead 1995; Dewar and Huang 1995), the density difference of this single box model can have the same value of density for two different values of Q if appropriate values of βS^{**} , αT^{**} , and τ_T and τ_S are used.

As Dewar and Huang (1995) also pointed out, this density difference can be thought of as a torque that forces circulation in a loop model for

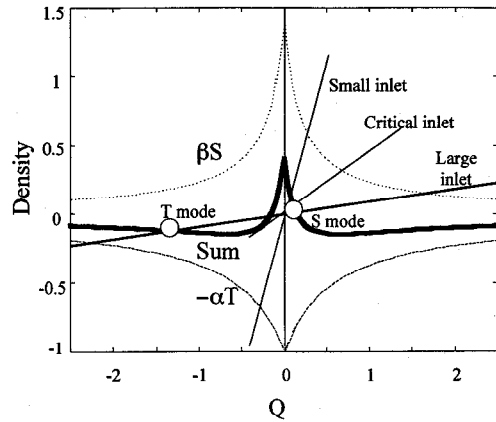


Fig. 2. Curves showing density due to salinity, temperature and their sum (bold curve, from equation 2.11) as a function of box flushing rate flushing rate Q . The three straight lines represent three possible dynamic relations at the inlet of the estuary. If the inlet is small, the flushing is small for given density and only the salinity driven state (denoted by S mode) is possible. Multiple states are found only if the density curves and straight line intersect at more than one point. There is a critical size whereby the dynamics at the mouth allows the dynamic relation to touch the bold curve on the left. For a large inlet, there is both a temperature and salinity mode.

this problem. Figure 2 also includes a straight line representing very simplified dynamics at the mouth of the estuary, which is that volume flux is linearly proportional to that torque. The line intersects the density curve at three points. Just as in the original two box model of Stommel 1961, two of these are stable points and represent two states of motion for the same forcing conditions. The third point is unstable so the time derivatives bring the solution from the vicinity of this point to one of the other two.

Given fixed values of τ_S , τ_T , α , and β , there are many values of T^{**} , S^{**} , and slope C (from the relation $Q = C\Delta\rho$) that do not lead to three points of intersection of the curves with a straight line. To get three points, two conditions are required, and these will be described next. They are subsequently used to determine whether this one box model could be applied to an open system such as an estuary.

The first criterion is that $\Delta\rho$ must be both positive and negative. For this to be true, it must change sign at some value of $|Q|/V$. Since $\Delta\rho$ is the sum of two hyperbolae which decay monotonically as $|Q|/V \rightarrow \infty$, the two derivatives can be equal in magnitude at only one point, which is a density extremum. Moreover $\Delta\rho$ approaches zero as Q approaches infinity, so a density extremum implies two values of Q for the same $\Delta\rho$. Thus the composite curve must cross $\Delta\rho = 0$. Using Eq. 2.11, the condition for $\Delta\rho/\rho = 0$ is

$$\frac{\beta S^{**}}{1 + \frac{|Q|\tau_s}{V}} = \frac{\alpha T^{**}}{1 + \frac{|Q|\tau_T}{V}} \quad (2.12)$$

Inverting both sides and rearranging

$$\frac{|Q|}{V} = \frac{\beta S^{**} - \alpha T^{**}}{\tau_s[\alpha T^{**} - \epsilon \beta S^{**}]} \quad (2.13)$$

where $\epsilon = \tau_T/\tau_s$. Since $|Q|/V$ must be positive, the following conditions must be met:

$$|\alpha T^{**}| < |\beta S^{**}| < \frac{\tau_s}{\tau_T} |\alpha T^{**}| \quad (2.14a)$$

or

$$\frac{\tau_s}{\tau_T} |\alpha T^{**}| < |\beta S^{**}| < |\alpha T^{**}| \quad (2.14b)$$

and $S^{**} T^{**} > 0$. These conditions are necessary for density to have both signs and thus necessary for multiple states to exist. But they are not sufficient conditions for multiple states to exist.

The second condition is that the flux law relating flow at the mouth of the estuary to density difference between estuary and ocean intersect this density curve at more than one point. For simplicity, we express this flux law as a linear relation $Q = C\Delta\rho/\rho$. Obviously there is a range of values of C for which the line does not intersect the density curve at three points. Thus if we wish this line to intersect the density curve,

$$C \geq \frac{\rho|Q|}{\Delta\rho} \Big|_{\text{Crit}} \quad (2.15)$$

where $(|Q|/\Delta\rho)|_{\text{Crit}}$ is the critical value where the straight line is tangent to Eq. 2.11 as sketched in Fig. 2. This is most easily expressed using the condition on the reciprocal, that is,

$$C^{-1} \leq \frac{\Delta\rho}{\rho|Q|/V} \Big|_{\text{Crit}} = \frac{d\Delta\rho}{\rho d|Q|/V} \quad (2.16)$$

Thus, using Eq. 2.11, setting aside the absolute value sign, and using the equality

$$\begin{aligned} & \left[\frac{\beta S^{**}}{1 + \frac{Q\tau_s}{V}} - \frac{\alpha T^{**}}{1 + \frac{Q\tau_T}{V}} \right] \\ &= \frac{-\beta S^{**}\tau_s Q}{V\left(1 + \frac{Q\tau_s}{V}\right)^2} + \frac{\alpha T^{**}\tau_T Q}{V\left(1 + \frac{Q\tau_T}{V}\right)^2} \end{aligned} \quad (2.17)$$

which is the cubic equation

$$\begin{aligned} & \left(\frac{Q}{V}\right)^3 + \left(\frac{Q}{V}\right)^2 \left[\frac{\beta S^{**}\tau_T(\tau_T + 4\tau_s) - \alpha T^{**}\tau_s(\tau_s + 4\tau_T)}{2\tau_T\tau_s(\beta S^{**}\tau_T - \alpha T^{**}\tau_s)} \right] \\ &+ \frac{Q}{V} \left[\frac{(\beta S^{**} - \alpha T^{**})(\tau_T - \tau_s)}{\tau_T\tau_s(\beta S^{**}\tau_T - \alpha T^{**}\tau_s)} \right] \\ &+ \frac{\beta S^{**} - \alpha T^{**}}{2\tau_T\tau_s(\beta S^{**}\tau_T - \alpha T^{**}\tau_s)} = 0 \end{aligned} \quad (2.18)$$

This has three roots, and if we take the values and insert them into Eq. 2.15 using Eq. 2.11, we get a criterion for C .

A Laboratory Experiment

Although the multiple states have been studied in numerous box-model and ocean circulation computer models, they have not previously been observed in a physical system, either in the laboratory or in nature. In the process of designing a laboratory experiment to view these effects, it became clear that only one box was needed. The application to estuarine processes then became obvious.

The experiment was designed as a table top physics experiment and some of the results are reported elsewhere (Whitehead 1996). It was intended to duplicate the simple conceptual model of Stommel (1961). In that model two side-by-side boxes were connected by two horizontal tubes—one at their top and one at their bottom. Temperature and salinity changes to water in the boxes were forced by diffusion through the walls. In addition, water within the box was well mixed. The salinity and temperature relations were very similar to those in the section Formulation.

That very simple model was apparently the first to show that there were three possible steady states of motion within a certain range of forcing parameters. One state was characterized by salinity dominating the density difference between basins. The second had temperature dominance. Both of these states were linearly stable, so small perturbations to the steady motion that was driven by the density difference between basins decayed in time. The third steady state was unstable and flow evolved to one of the other two states.

The apparatus (Fig. 3) consisted of a $10 \times 10 \times 8$ cm deep watertight "test chamber" (estuary), that was a plexiglas box with 1" thick styrofoam thermal insulation on the sides and top. The bottom of the chamber was a copper plate in contact with hot bath water of temperature T_b . The water surface inside the chamber was in contact with a flat horizontal common household sponge. Salt water with density 1.006 g cc^{-1} was pumped into the sponge top by a precision pump at a rate of

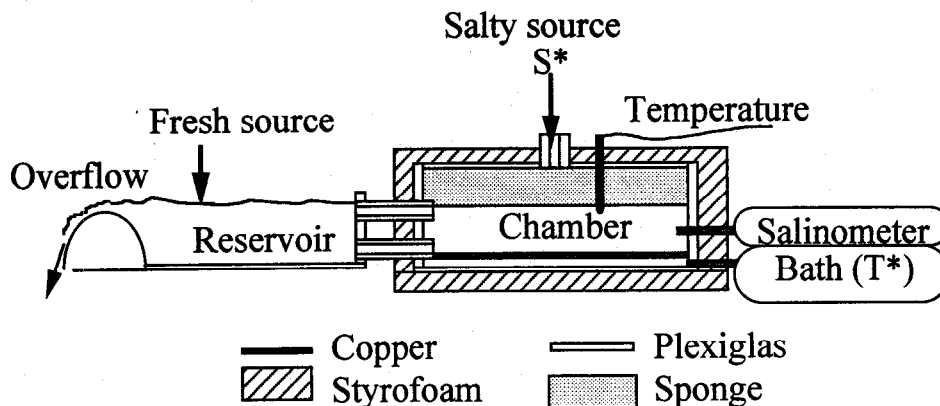


Fig. 3. The laboratory apparatus used to observe multiple states in a single chamber.

0.2 cc s^{-1} . The water in the test chamber was heated from below and subjected to a flux of high salinity water from above. This has the effect of mixing the test chamber water vertically, since temperature decreases density while salinity flux increases it. On one side wall of the chamber were two horizontal tubes 1.3 cm i.d. and 14 cm long. The centerline of one tube was 1.0 cm above the copper plate. The centerline of the other was 3.5 cm above the copper plate and directly over the first tube, so the two tubes allowed convection flow of water between the chamber and an outer reservoir (ocean) containing fresh water at room temperature. Convection would produce flow into the chamber through one tube and out the other, the direction depending on the density of the water in the test chamber. The reservoir was $50 \text{ cm} \times 50 \text{ cm} \times 5 \text{ cm}$ in size. The freshness of its water was assured by an inflow of de-aerated water at the rate of $1\text{--}2 \text{ cc s}^{-1}$. The excess water from inflow into the chamber was removed by outflow over a weir. Reservoir water was flushed gently by a thermostatic bath that maintained the water at 21°C . The flushing was gentle enough to prevent interference with the flow through the two tubes, but it was strong enough to mix the reservoir.

The apparatus is a good first approximation to one of the containers in Stommel's 1961 study. In the absence of both thermal forcing and exchange with the reservoir, the chamber's salinity obeys the relaxation equation

$$dS/dt = q(S - S_p)/V$$

where q is volume flux of water with salinity S_p into the chamber and V is volume of the chamber. We have assumed water flows out of the chamber with flux q . Temperature obeys a similar type of relaxation equation in the absence of both salinity forcing and exchange with the ocean. Temperature relaxation time depends on the Nusselt number of

the Rayleigh-Benard convection that is produced by heating from below. Our laboratory measurements indicate the salinity relaxation time V/q is approximately 2,000 s and that this is approximately four times larger than the thermal relaxation time of 500 s.

It was necessary to measure and calculate very accurately the change of density due to both salinity and temperature. Temperature data from one thermistor in the chamber and from one in the reservoir, and density data from an Anton Paar densimeter (accurate to four significant figures) were recorded every 30 s or 60 s for the duration of each run. The contributions of temperature variation and of salinity change to the density difference between the chamber and the reservoir were then separately determined. The density difference due to temperature was calculated from the temperature records using chamber and reservoir temperatures corrected to an absolute accuracy of 0.1°C . Values of density of seawater for assorted values of temperature and salinity from Fofonoff and Millard (1983) were then used to calculate density difference between chamber and reservoir using least squares fit. Two terms in the temperature series were used in this estimate. The neglected third-order terms were at most 0.0002 g cm^{-3} . A linear effect of salinity variation to the coefficient of thermal expansion was included, but higher order terms were not. Although we used sea salt tables rather than sodium chloride tables, direct comparison of density values reveals the difference between sea salt and sodium chloride to the coefficient of thermal expansion results in a density error of only a few percent of 0.0002.

To measure density due to salinity, water from the test chamber was continuously circulated from the test chamber to the densimeter and back. The pumping rate was slow enough (0.01 cc s^{-1}) so that the temperature of the water sample in the den-

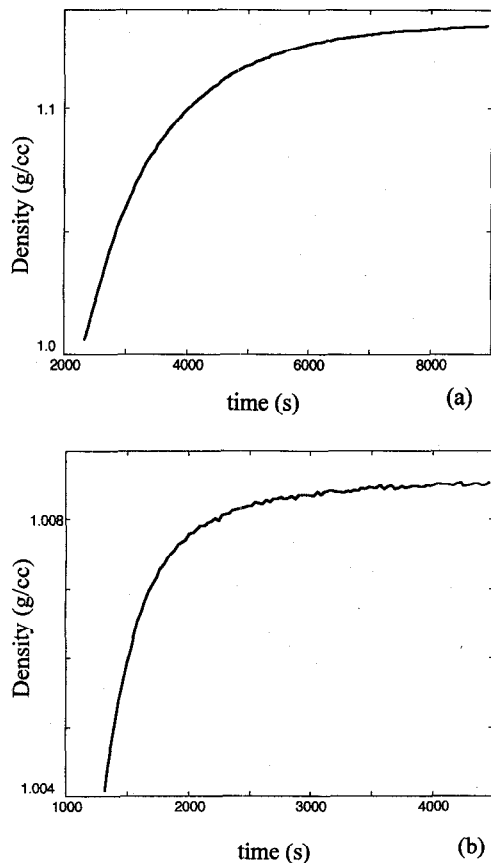


Fig. 4. Measurements to determine time constants of salinity and temperature. a) Response of density from changes in salinity within the box after initiation of the pump. b) Response of density due to change in temperature in the box after initiation of the temperature bath.

siometer had reached the temperature of the test chamber, 20°C. Thus the densimeter recorded directly the density due to only salt in the chamber. Error due to the effect of temperature variation from 20°C on the measurement of density is less than 0.0002. Finally, the density due to salinity of samples of the reservoir water was measured after the experimental run and was subtracted from the densimeter readings. It was important to do this as corrections ranged up to 0.0010 g cm⁻³.

To measure the salinity decay time, two stoppers were placed in the two tubes. The top stopper was given a small hole to allow outflow of the added volume. Density was recorded over time at a constant T^* . The response is shown in Fig. 4a. The curve is close enough to an exponential decay to indicate that the salinity relaxation time is approximately 2000 s, which is in rough agreement with the estimated time $V/q = 1,500$ s. Thermal decay time of the chamber was measured by recording temperature response over time to a sudden change in T^* for constant S . This response is

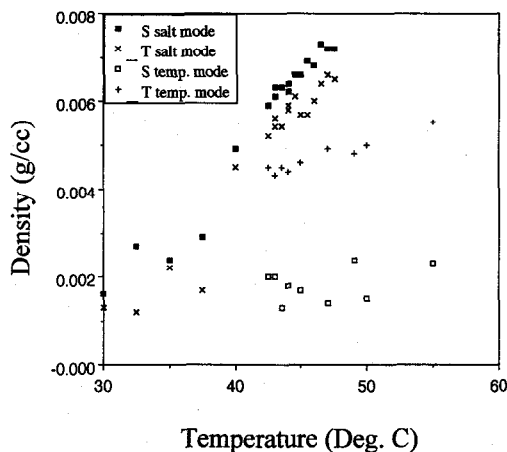


Fig. 5. Density due to salinity and to temperature for 27 steady experiments. The squares denote density difference between chamber and reservoir due to salt while the chamber was in the salt mode (solid) and temperature mode (open). The pluses denote the absolute value of density difference between chamber and reservoir due to temperature difference while in the salt mode. The x's give the same while in the temperature mode.

shown in Fig. 4b. It is also close to an exponential decay, with the time constant of about 500 s.

Following the apparatus calibrations, about 60 (including preliminary) experimental runs were conducted. Each run was conducted by adjusting bath temperature and allowing at least 3 h for the bath to come to steady state. The volume flux and salinity of the steadily injected water was kept the same in every run. Temperature of the bath below the copper plate was fixed for each run but was varied over a wide range from run to run. The experiment arrived at values that were very close to steady final values within 3 h. It would take many more hours to become steady to the last digit (one part in 10⁴); some runs were left for 24 h.

The steady-state densities due to both temperature and salinity in the chamber for all runs are shown in Fig. 5. Plotted are values of density due to temperature and salinity as a function of bath temperature. It is clear that there are two trajectories for the temperature and salinity density pairs. At lower bath temperature, density due to both salinity and temperature increases with bath temperature. In addition, density due to temperature is roughly 0.0010 units less than density due to salinity, so the chamber is in the salt-mode. These two trajectories in the data terminate at a bath temperature of 48°C. Above this value, data pairs only lie in the other trajectory pair. This second pair of trajectories exhibits significantly less dependence of density on bath temperature. Densities were also smaller in magnitude than the first pair. Density due to temperature is slightly smaller

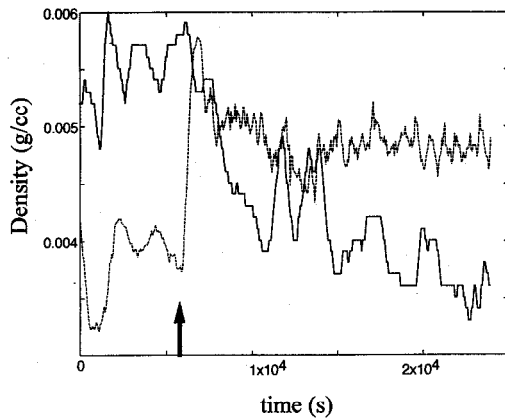


Fig. 6. Plot of density to salinity (solid) and temperature (dashed) during an individual transient run. Temperature of the bath was suddenly increased from 41°C to 50°C at 5700 s (large arrow). The spike in salinity during transition is obvious.

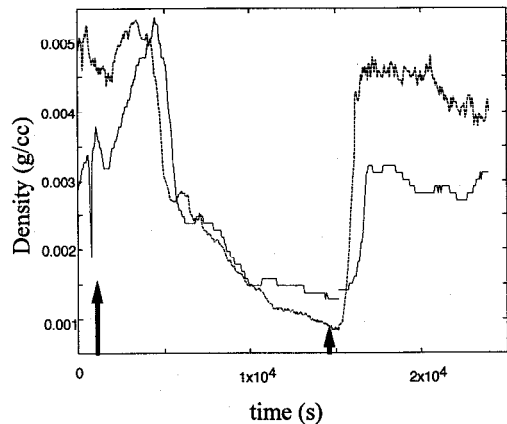


Fig. 7. Plot of density due to salinity and temperature recorded during transition from temperature to salt mode and then back again. Temperatures of the bath was decreased from 50°C to 20°C at 1020 s (large arrow) and increased back to 50°C at 14520 s (small arrow).

than the density due to temperature when in the salt mode. But density due to salt is much smaller than its value in the temperature mode. In addition, density due to temperature was more than a factor of two greater than density due to salt.

All these features are in qualitative agreement with the single box theory developed here and the double box theory of Stommel (1961). In the salt-driven mode, density difference between salt and temperature is small. Temperature, being the property with the fast time constant, is close to the temperature of the bath. Density due to salinity is just a little (few percent) greater than density due to temperature. In contrast, when flow is in a temperature-driven mode, the rate of flushing is greater and the flow is of opposite sign. Temperature is significantly less than bath temperature. Density due to temperature is correspondingly smaller than its value in the salt mode. But density due to salinity is very much smaller due to the vigor of the flushing. Density due to temperature is greater by a factor of 2 or so, than density due to salinity. The absolute value of this difference is greater than the absolute value of the density difference when the flow in the box is in the salt mode at the same parameters.

The rate of flushing could also be directly observed through injecting and timing movement of a small amount of dye near each tube connecting the chamber to the reservoir. For cases when the temperature and salinity data indicated a salt mode, there was a very slow trickle of salty water out of the bottom tube (from box to reservoir) and very slow inflow into the top tube.

In contrast, when the water in the box was in the temperature-driven mode, inflow was visibly faster and always with the opposite sense. Flow of fresh

water was from reservoir to chamber through the bottom tube and from chamber to reservoir through the top. The speed of the injected dye plume along the tygon tube was clocked a number of times and was seen to be roughly five to ten times greater than salt-mode speeds. Speeds were not routinely obtained for all runs, and no quantitative comparison of velocity was obtained over the entire range of the experiments.

It was obvious that the plumes of heated salty water coming from the chamber into the reservoir were extremely prone to double-diffusion. If the chamber was in the salt-mode, the very hot salty plume entering the reservoir would rapidly lose some of its heat by conduction to surrounding fresher water. A typical salt plume containing dye for visualization would remain at the bottom of the basin, but it would be surrounded by convection cells rising upward and containing small wisps of dye. If the chamber was in the temperature-mode, the slightly salty but very hot plumes would float along the top of the reservoir water but would exhibit salt fingers that apparently transported salt into the fresh water. Some of the hot slightly salty water appeared to sink in bulk after it was cooled by the air.

Additional transient experiments were made by suddenly changing the temperature of the bath. Data recorded every 30 s are shown in Fig. 6 for suddenly increasing temperature and in Fig. 7 for suddenly decreasing temperature with a subsequent increase. Since velocity must change sign in switching modes, chamber temperature and salinity is expected to temporarily increase during the switch. A salinity spike showing this temporary increase is clearly visible in the data. The tempera-

ture spike is not visible. Probably it is hidden in the large temperature change from the baths.

Consequences

The experiment essentially verified the predictions of the well-known box models in every way. Two states existed over a range of forcing parameters. The salt, or long-time-scale dominated state has large values of density in the box, with the salt density slightly greater than temperature. The temperature, or short-time-scale state has lower densities, large density differences, and greater exchange velocities.

The only new aspect of this work is the realization that the above effects can happen for one box next to a neutral body of water. This opens up the possible applications of these concepts to estuaries, coastal shelf waters, and marginal seas. Possibly, in the rich variety of situations all over the world, many examples of multiple states and the transition from one to the other can be found.

The criteria we have discussed illustrate the role of the time constants and the role of the dynamics of the exchange mechanism between the basin and the ocean. To find how to apply the models to real estuaries, let us consider again Eq. 2.3 and Eq. 2.4:

$$\frac{dS}{dt} = \frac{1}{\tau_s}(S^{**} - S) - \frac{|Q|}{V}S \quad (4.1)$$

$$\frac{dT}{dt} = \frac{1}{\tau_T}(T^{**} - T) - \frac{|Q|}{V}T \quad (4.2)$$

To find the conditions that must be met for multiple states, we first determine the values of density and Q/V at a density minimum (if one exists). Assuming Q is positive, we take the derivative of Eq. 2.11 with respect to Q/V , and set it to zero to produce a condition at the density minimum of

$$\frac{\alpha T^{**}\tau_T}{\left(1 + \frac{\tau_T Q}{V}\right)^2} - \frac{\beta S^{**}\tau_s}{\left(1 + \frac{\tau_s Q}{V}\right)^2} \quad (4.3)$$

which gives a value of

$$\frac{Q}{V} = \frac{1}{\sqrt{\tau_T\tau_s}} \left[\frac{\sqrt{\beta S^{**}} - \sqrt{\epsilon\alpha T^{**}}}{\sqrt{\alpha T^{**}} - \sqrt{\epsilon\beta S^{**}}} \right] \quad (4.4)$$

since Q is positive this requires

$$\frac{1}{\epsilon} > \frac{\beta S^{**}}{\alpha T^{**}} > \epsilon \quad \text{for } \epsilon < 1 \quad (4.5)$$

or

$$\frac{1}{\epsilon} < \frac{\beta S^{**}}{\alpha T^{**}} < \epsilon \quad \text{for } \epsilon > 1 \quad (4.6)$$

where $\epsilon = (\tau_T/\tau_s)$. Assuming $\epsilon \ll 1$,

$$\frac{Q}{V} \cong \sqrt{\frac{\beta S^{**}}{\tau_s\tau_T\alpha T^{**}}} \quad (4.7)$$

For this case,

$$\frac{\Delta\rho_{\min}}{\rho} = \frac{\beta S^{**}}{1 + \frac{\sqrt{\beta S^{**}}}{\sqrt{\epsilon\alpha T^{**}}}} - \frac{\alpha T^{**}}{1 + \frac{\sqrt{\epsilon\beta S^{**}}}{\sqrt{\alpha T^{**}}}} \quad (4.8)$$

Expanding as a power series in $\sqrt{\epsilon}$,

$$\frac{\Delta\rho_{\min}}{\rho} \cong -\alpha T^{**} + 2\sqrt{\epsilon\alpha T^{**}\beta S^{**}} + 0(\epsilon)$$

If an estuary, shelf, or marginal sea has an opening that allows a volume flux greater than the value given by Eq. 4.7, using a density difference given by Eq. 4.8, it would have multiple states. This is a sufficient condition for multiple states. A necessary and sufficient condition for multiple states involves setting $\Delta\rho V/Q$ equal to $V d\Delta\rho/dQ$, and using that to determine a value of Q/V and $\Delta\rho$ required by an opening. The solution is algebraically much more complicated as shown in Formulation.

In assessing possible values appropriate for natural features, let us estimate a typical thermal response time using the time it takes to cool a shallow bay by 10°C with a relatively large value of heat flux typical of wintertime cooling, say $H = 500$ watts m^{-2} . Using a water depth of $D = 10$ m, density of 10^3 kg m^{-3} , and specific heat $C_p = 4.1 \times 10^3$ j/°C kg, we get a cooling time scale which we set equal to time constant τ_T of

$$\begin{aligned} \tau_T &= \frac{\rho C_p \Delta T D}{H} = 8 \times 10^5 \text{ s} = 9.25 \text{ days} \\ &\cong 10^6 \text{ s} \end{aligned} \quad (4.9)$$

Let the salt time constant be found assuming a relatively moderate river with volume flux of 100 m^3 s^{-1} , flowing into a very large estuary (like Chesapeake Bay) of volume 10^{11} m^3 (10 m \times 100 km \times 100 km), so $\tau_s \cong 10^9$ s \cong 30 yr. Let $\beta S^{**} = 0.02$ (freshwater inflow to region with outer ocean about 28‰ using $\beta \cong 0.71 \times 10^{-3}$ kg/1‰ and $\alpha T^{**} = 0.002$, which assumes a wintertime temperature about 10°C cooler than the surrounding ocean). Then Eq. 4.8 gives

$$\Delta\rho_{\min} = -2 \text{ kg } m^{-3} \quad (4.10)$$

The value Q/V that this gives is found using Eq. 4.7

$$\frac{Q}{V} = 3.4 \times 10^7 \text{ s}^{-1} \quad (4.11)$$

which corresponds to a residence time of about 30 d. Using a volume of 10^{11} m^3 , Eq. 4.11 gives $Q =$

TABLE 1. Typical values of freshwater runoff volume flux, depth, area, volume, saltwater time constant, temperature time constant and critical flushing rate for various basins.

	q $\text{m}^3 \text{s}^{-1}$	D m	A m^2	V m^3	t_s s	t_T s	Q_c $\text{m}^3 \text{s}^{-1}$
Estuary	1	10	10^6	10^7	10^7	10^6	10
Bay	10^2	10	10^{10}	10^{11}	10^9	10^6	10^4
Shelf/km	1	10^2	10^8	10^{10}	10^{10}	10^7	10^2
Small sea	10^3	10^2	10^{11}	10^{13}	10^{10}	10^6	3×10^5
Large sea	10^4	3×10^2	10^{13}	3×10^{15}	3×10^{11}	10^7	5.7×10^6

$3.4 \times 10^4 \text{ m}^3 \text{ s}^{-1}$. We have not discussed the detailed dynamics of the flushing process through the inlet between the basin and the ocean. But if the dynamics allow a volume flux of more than $3.4 \times 10^4 \text{ m}^3 \text{ s}^{-1}$ from a forcing density difference of about 0.002, the system could have multiple states. Consider the nonrotating lock-exchange formula (Yih 1988, p. 207)

$$Q = \frac{1}{4} \sqrt{g \frac{\Delta \rho}{\rho}} D^{3/2} W \quad (4.12)$$

where W is the width of a mouth. Using the above numbers for Q , $\Delta \rho$, and D ,

$$W > 30 \text{ km} \quad (4.13)$$

would produce a volume flux greater than that given by Eq. 4.11, and this would produce multiple states. Thus, a reasonably mouth-width is indicated. If W is much smaller than 30 km, the maximum wintertime cooling would produce a density difference much smaller than the relatively steady salinity-driven density difference so only a salt mode could exist in a steady state. Such a situation is typical, for instance, of conditions in many fjords.

It is notable that many enclosed seas are salt or fresh-water dominated. Examples are the Mediterranean, the Black Sea, and the Baltic Sea. The above analysis indicates that the salt water balance must hold in these seas because their openings to the ocean are too small for the faster thermal forcing to hold. Large estuaries, such as Chesapeake Bay, and Delaware Bay, also appear to be so limited.

Such salient features of other basins with various sizes are listed in Table 1. For these examples we took $\beta S^{**} = 3 \times 10^{-2}$ and $\alpha T^{**} = 3 \times 10^{-3}$. In all cases Eq. 4.8 was used to determine that a density minimum was produced. The value of volume flux at the density extremum Q_c was calculated using Eq. 4.7, so $Q_c = 3V/\sqrt{\tau_s \tau_T}$. The interpretation of Q_c is that it is the minimum volume flux at the mouth of the estuary needed from a density difference given by Eq. 4.8 for multiple states to be possible. Since the inlet conditions have not yet been specified, we can now inquire into what inlet conditions would produce of flux in excess of Q_c .

The estuary example assumes a small stream flowing into a region 1 km^2 . The salt time constant is about 100 d and the temperature constant is about 10 d. The required value of Q_c at the mouth is only $10 \text{ m}^3 \text{ s}^{-1}$. Using the density difference from temperature and Eq. 4.12 we find that an inlet width, W , greater than 7.3 m would produce multiple states.

The bay is considerably larger, at $100 \text{ km} \times 100 \text{ km}$, but of the same depth. It is similar to the bay which was used for the first calculation (Eqs. 4.9 to 4.11) in this section, and like that example there is a moderate river feeding in fresh water. Q_c is $10^4 \text{ m}^3 \text{ s}^{-1}$, so using Eq. 4.12 we find that bays with mouth widths greater than 7.3 km could have multiple states, and smaller ones would be in the salt mode only.

The shelf has the same properties of the bay per unit kilometer, but it is 10 times deeper. This makes the equivalent volume greater than the bay example, but time scales are each 10 times greater, so that Q_c is equivalent to the bay example. However, the rates of exchange between continental shelf water and the deep sea are not measured or understood.

The small sea is $100 \text{ km} \times 1,000 \text{ km}$ and is again 100 m deep. Volume flux must be greater than approximately $Q_c = 0.3 \text{ Sv}$ to have multiple states. The large sea is 300 m deep and $1,000 \text{ km} \times 10,000 \text{ km}$ in area. It corresponds to a number of marginal seas such as the Black Sea, the Mediterranean Sea, and the Arctic Ocean (Aagaard and Carmack 1989; Hunkins and Whitehead 1992). All these are in the salt mode and the volume fluxes at their openings are less than the critical value of $Q_c = 5.7 \text{ Sv}$ calculated here, so it is unlikely they could possess multiple states.

These examples are only suggestive. More complicated modeling studies may uncover exceptions to these general statements. It is hoped that this picture will stimulate further field and modeling studies.

Let us summarize by looking at explicit values more closely. Typically an estuary fed by freshwater runoff will have a value of βS^{**} given by the difference between freshwater and seawater, which is

at most 3×10^{-2} , although estuaries situated in continental shelf regions with low salinity offshore water could have smaller values. Since typical temperature differences between estuary and ocean are about 20°C at most, αT^{**} for typical salt water cannot be greater than about 3×10^{-3} . This satisfies the left-hand part of Eq. 2.14a, but for two signs of density to be possible, $\tau_s \alpha T^{**} / \tau_T \beta S^{**} > 1$. Since αT^* is about an order of magnitude less than βS^{**} , τ_s must be about an order of magnitude greater than τ_T for multiple states. This is always possible given sufficiently small freshwater flow into the estuary, since Eq. 2.5 defines $\tau_s = V/q$. Typically it takes a few days to change temperature significantly in an estuary, so setting τ_T to be about 10^6 s, we see that typically $\tau_s \gg 10^6$ s for multiple states. This means that for every $1 \text{ m}^3 \text{ s}^{-1}$ of freshwater flowing into an estuary, the volume of the estuary should be about 10^6 m^3 or more. If this is not met, the estuary will have salinity-dominated density irrespective of the rate of flushing in the mouth. Most estuaries satisfy this criterion for multiple states. Estuaries in coastlines fed by small watershed regions such as those on islands or peninsulas are thus strongly suited for multiple states compared to those next to large continents with their large rivers.

Although the requirement $\tau_s \gg 10^6$ S is almost always satisfied regardless of either the size of the estuary or the dynamics at the mouth of the estuary, the second requirement discussed in Formulation, that volume flux at the mouth be greater than a certain amount (Eq. 2.16) also must be met. Let us investigate the case of $\tau_s \gg \tau_T$, for which Eq. 2.17 reduces to

$$\alpha T^{**} = \frac{\beta S^{**} V}{Q \tau_s} \quad (4.14)$$

so

$$\frac{Q}{V} = \frac{\beta S^{**}}{\alpha T^{**} \tau_s} \quad (4.15)$$

with the value of density difference of

$$\frac{\Delta \rho}{\rho} = \alpha T^{**} \quad (4.16)$$

Thus, if at the mouth of the opening

$$C \geq \frac{\beta S^{**} V}{(\alpha T^{**})^2 \tau_s} \quad (4.17)$$

(see Eq. 2.15), multiple states are possible. But we have the simple definition of $\tau_s = V/q$, so if the mouth dynamics are such that

$$|Q| \geq \frac{\beta S^{**} q}{\alpha T^{**}} \quad (4.18)$$

for

$$\frac{\Delta \rho}{\rho} = -\alpha T^{**} \quad (4.19)$$

and $\tau_s > 10 \tau_T$ (using $\alpha T^{**} = 10^{-3}$, $\beta S^{**} = 10^{-2}$), then multiple states are possible.

Let us consider three candidate dynamical laws to govern buoyancy-driven flow through the mouth of the estuary. First, frictional flux is

$$Q = \frac{g \Delta \rho D^4 W}{12 \rho \nu L} \quad (4.20)$$

when L is length of the mouth and ν is (possibly turbulent) viscosity. Second, inertial exchange flow (as in Eq. 4.12) is

$$Q = \frac{1}{4} \sqrt{g \frac{\Delta \rho}{\rho}} D^{3/2} W \quad (4.21)$$

and a third is a rotating inertial exchange flow

$$Q = \frac{1}{6} \left| \frac{g \Delta \rho}{\rho} \right| \frac{D^2}{f} \quad (4.22)$$

(Bye and Whitehead 1975) where f is the Coriolis parameter.

In the first case, using $\nu = u^* D/2$ with $u^* = 1 \text{ m s}^{-1}$ (say, from tidal currents), $\beta S^{**} / \alpha T^{**} = 10$, $\Delta \rho / \rho = |\alpha T^{**}| = 10^{-3}$, (these values will be used in the next three examples (through Eq. 4.27)) and using Eq. 4.20 with Eq. 4.18, we get

$$1.7 \times 10^{-3} \frac{D^3 W}{L} > 10q \quad (4.23)$$

In the town of Falmouth there are a number of finger ponds connected to Vineyard Sound by narrow openings. Because the Cape Cod watershed produces very small streams, a typical pond such as Green Pond is fed by perhaps $0.01\text{--}0.1 \text{ m}^3 \text{ s}^{-1}$ of fresh water. Moreover tides are weak so tidal currents are on the order of 10 cm s^{-1} . Let us use an opening depth $D = 4 \text{ m}$, width $W = 20 \text{ m}$, and length of the shallow opening $L = 10 \text{ m}$. Using $q = 0.01 \text{ m}^3 \text{ s}^{-1}$, the criterion given by Eq. 4.23 is $0.2 > 0.1$ and is met. This is an extreme case, since we have used a very small value of freshwater inflow. Frictional effects may decrease the left-hand side for such a case and cause the inequality to be violated. In addition, we have used the smallest value of q . So there are a number of reasons why the inequality might be violated, in which case the estuary would always be freshwater driven. Next, take $q = 1 \text{ m}^3 \text{ s}^{-1}$, an estuary with a depth of 6 m , and an opening 100 m long, then the mouth would have to be over 2.7 km wide, which could be satisfied by some estuaries. Greater depth or smaller river flow would make it easier to fit the criterion.

Deeper estuaries, with depths of order 10 m will

meet the criteria more easily (as shown in Table 1). But as depth increases above a few meters the effect of friction drops off because stratification quenches the turbulence and inertial exchange limits the flow. In that case, Eq. 4.21 in Eq. 4.18 gives

$$\frac{1}{4\sqrt{\frac{g\Delta\rho}{\rho}}} D^{3/2} W > 10q \quad (4.24)$$

or

$$0.025 D^{3/2} W > 10q \quad (4.25)$$

For $D = 10$ m and $\alpha T^{**} = 10^{-3}$ with $q = 1$ m³ s⁻¹

$$W > 12.6 \text{ m} \quad (4.26)$$

which is easily satisfied for a variety of estuaries. Finally, for greater depth and width, the effects of the Earth's rotation begins to limit the flow to a front that extends across the mouth of the opening. This happens when width exceeds a Rossby radius

$$R_0 = \frac{1}{2f\sqrt{\frac{g\Delta\rho D}{\rho}}} \quad (4.27)$$

which for a depth of $D = 10$ m is $R_0 = 1.6$ km. If W is greater than R_0 , we use Eq. 4.25 with R_0 substituted for W , which gives $q < 126$ m³ s⁻¹.

For evaporative estuaries the results are slightly different. Since q is negative, Eq. 2.3 for salinity is replaced by

$$\frac{dS}{dt} = \frac{1}{\tau_s} (S^{**} + S) - \frac{|Q|}{V} S \quad (4.28)$$

with solution

$$S = \frac{S_0}{\frac{|Q|}{q_e} - 1} \quad (4.29)$$

where q_e is the volume flux of water evaporated and S_0 is salinity of the ocean. The only sensible solutions are for $|Q| > q_e$ so that as $|Q|$ approaches q_e the salinity becomes saturated. In addition, τ_s may be large in practice, of order 10^9 s or 10^{10} s as it is the time needed to evaporate all water from the basin. Such basins may then require $|Q|$ significantly greater than $10q_e$. To insert some test numbers, consider a 3-km² estuary with surface evaporation of 0.1 m mo⁻¹ which gives a removal rate of about 0.1 m³ s⁻¹. A frictional opening 10 m deep with $L = 100$ m, $W = 120$ m, and using $\Delta\rho/\rho = 10^{-3}$ would produce $Q = 1$ m³ s⁻¹ and thus would flow enough to produce three states. In addition, at such a depth the inertial mechanism 4.21 may be required, in which case the opening would produce a flow of 9.5 m³ s⁻¹. In that case, if width

exceeds a Rossby radius of 1.5 km, flux will be clearly greater than that needed for multiple states.

Figures are available for Spencer Gulf, South Australian (Bullock 1975; Bye and Whitehead 1975). Using a depth of 40 m, $\alpha T^{**} = 4 \times 10^{-1}$, $q_e = 6 \times 10^3$ m³ s⁻¹; and an area of 1.2×10^{10} m², we find $\tau_s = 8 \times 10^8$ s, so by Eq. 4.18 if $Q > 10^4$ m³ s⁻¹, multiple states may be possible. Using Eq. 4.21, we get $Q = 1.3 \times 10^4$ m³ s⁻¹, so it is just above the limit and a temperature mode may be possible. Spencer Gulf seems to be locked in the salty mode at present, but it could change from extreme freshening by rain or from extreme heating. The actual criteria need to be reworked in greater detail for an evaporative basin, however, and this remains unresolved.

In summary, estuaries with buoyancy-driven inlets which are driven by both temperature and salinity differences between estuary and deep ocean can have either temperature or salinity as the dominant driving. Naturally, if one driving is very much greater than the other it will predominate. If they are roughly equal, either can predominate, depending upon the relative time constants. Usually salinity possesses a greater time constant within basins. In that case, if $\beta S^{**} > \alpha T^{**}$, estuaries with relatively small openings will be salinity driven, those with large openings will be temperature driven, and there is a range of multiple stable stationary states where either can drive the flow, depending on initial conditions.

For multiple states it is necessary that Eq. 2.14a be satisfied

$$|\alpha T^{**}| < |\beta S^{**}| < \frac{\tau_s}{\tau_r} |\alpha T^{**}|$$

and the other condition needed is that for multiple states

$$\frac{\rho|Q|}{\Delta\rho} \Big|_{\text{crit}} > \frac{\beta S^{**} V}{(\alpha T^{**})^2 \tau_s} = \frac{\beta S^{**} q}{(\alpha T^{**})^2}$$

otherwise salinity dominates. We have investigated the possible magnitudes of such quantities for a number of examples, and find there may be such situations in nature.

ACKNOWLEDGMENTS

Thanks are due to John Salzig for construction of the apparatus. Research supported by the Office of Naval Research under contract N00014-97-1-0195, sponsored jointly by the coastal, polar, and physical oceanography sections. Woods Hole Oceanographic Institution contribution number 9577.

LITERATURE CITED

AAGAARD, K. AND E. C. CARMACK. 1989. The role of sea ice and other fresh water in the Arctic circulation. *Journal of Geophysical Research* 94:14,485-14,498.

- BYE, J. A. T. AND J. A. WHITEHEAD. 1975. A theoretical model of the flow in the mouth of Spencer Gulf, South Australia. *Estuarine and Coastal Marine Science* 3:477-481.
- BULLOCK, D. A. 1975. The general circulation of Spencer Gulf, South Australia for the period February to May. *Transactions of the Royal Society of South Australia* 99:43-57.
- DEWER, W. K. AND R. X. HUANG, 1995. Fluid flow in loops driven by freshwater and heat fluxes. *Journal of Fluid Mechanics* 297: 153-191.
- FOFONOFF, N. AND R. C. MILLARD, JR. 1983. Algorithms for Computation of Fundamental Properties of Sea Water. UNESCO Technical Paper in Marine Science, 44, UNESCO, Paris.
- HANSEN, D. V. AND M. RATTRAY, JR. 1966. New dimensions in estuary classification. *Limnology and Oceanography* 11:319-325.
- HUNKINS, K. AND J. A. WHITEHEAD. 1992. Laboratory simulation of exchange through Fram Strait. *Journal of Geophysical Research* 97:11,299-11,321.
- KENNISH, M. J. 1986. Ecology of Estuaries, Volume 1, Physical and Chemical Aspects. CRC Press, Inc., Boca Raton, Florida.
- KJERFVE, B. 1988. Hydrodynamics of Estuaries. CRC Press, Inc., Boca Raton, Florida.
- IPPEN, A. T. 1966. Estuary and Coastline Hydrodynamics. McGraw-Hill, Inc., New York.
- MAROTZKE, J. 1994. Ocean models in climate problems, p. 79-109. In P. Malanotte-Rizzoli and A. R. Robinson, (eds.), Ocean Processes in Climate Dynamics: Global and Mediterranean Examples.
- MIYAKE, H, I. TANAKA, AND M. TAKASHI, M. 1988. Outflow of water from Funka Bay, Hokkaido, during early spring, *Journal of the Oceanographical Society of Japan* 44:163-170.
- PRANDLE, D. (ED.). 1992. Dynamics and Exchanges in Estuaries and the Coastal Zone. American Geophysical Union, Washington, D.C.
- STOMMEL, HENRY. 1961. Thermohaline convection with two stable regimes of flow. *Tellus* 13:224-230.
- WEAVER, A. J. AND T. M. C. HUGHES. 1992. Stability and variability of the thermohaline circulation and its link to climate. *Trends in Physical Oceanography* 1:15-70.
- WHITEHEAD, J. A. 1995. Thermohaline ocean processes and models. *Annual Review of Fluid Mechanics* 27:89-113.
- WHITEHEAD, J. A. 1996. Multiple states in doubly driven flow. *Physica D* 97:311-321.
- WOLANSKI, E. 1988. Circulation anomalies in tropical Australian estuaries. Chapter 14 in Bjorn Kjerfve (ed.), Hydrodynamics of Estuaries, Volume II, Estuarine Case Studies. CRC Press, Boca Raton, Florida.
- YIH, C. S. 1988. Stratified Flows. Academic Press, New York.

Received for consideration, April 8, 1996
Accepted for publications, October 14, 1997